IPPI
Polyolefins Journal, Vol. 12, No. 1 (2025)
DOI: 10.22063/POJ.2025.35567.1329
ORIGINAL PAPER

Valorization of bagasse/polypropylene nanocomposites via nanosilica and mercerization treatments

Reza Naghdi*,[1], Tahereh Nejat[2]

[1]Department of Wood and Paper Science and Technology, Faculty of Natural Resources, Semnan University, Semnan 35196-45399, Iran
[2]Faculty of Chemical, Petroleum and Gas Engineering, Semnan University, Semnan, 35196-45399, Iran

Received: 8 October 2024, Accepted: 4 February 2025

ABSTRACT

The ever-increasing environmental constraints over waste disposal led us to study the feasibility of valorizing bagasse/ polypropylene composites via nanosilica and mercerization treatments. Water absorption and thickness swelling of the nanocomposites improved due to the barrier properties of nanosilica particles. FTIR spectra revealed decreased hydroxyl groups as well as carbonyl groups disappearance after alkali treatment. Except for impact strength, the combined nanosilica-mercerization treatment could enhance the mechanical performance of the biocomposites. Thermogravimetric analysis showed higher degradation temperatures and residual char yields after the combined nanosilica-mercerization treatment. Furthermore, differential scanning calorimetry indicated that the individual mercerization and nanosilica treatments had no distinct effect on the thermal performance of the composites, whereas the combined treatment brought about marked improvements in the given properties, e.g; melting and crystallization temperatures and crystallinity rate. The present study introduces a novel technique to valorize a totally waste-based bagasse/ polypropylene composite material holding a promising potential for various industrial applications. **Polyolefins J (2025) 12: 61-71**

Keywords: Waste plastic; sugar cane residue; nano SiO_2; alkalization; synergistic effects.

INTRODUCTION

Production of waste-based natural fiber polymer composites has globally gained significant attention in recent years [1-3]. The hygroscopic nature of wood fibers causes poor interfacial adhesion between the natural fibers and the polymer matrix creating favorable conditions for fungal attack [4-6]. Therefore, the surfaces of lignocellulosic fibers require treatment to reduce their hygroscopicity. Alkali treatment can dissolve wax, pectin, and lignin present on fiber surfaces, thus introducing more accessible hydroxyl moieties on natural fibers. The hydrogen bonds in cellulose and hemicellulose are broken due to the given treatment, leading to rough fiber surfaces. Alkali converts hydroxyl groups to RO^-, engendering reduced water absorption in natural fibers according to the following reaction [7,8]:

$$\text{Wood–OH} + \text{NaOH} \rightarrow \text{Wood–O-Na} + H_2O + \text{impurities (wax, pectin, and lignin)} \quad (1)$$

Mercerization has been reported to improve mechanical

*Corresponding Author - E-mail: Reza_naghdi@semnan.ac.ir

CC BY NC SA

performance, slenderness and surface fibrillation in lignocellulosic fibers [9]. Additionally, alkali treatment could improve thermal stability as a result of hemicellulose dissolution, being the most thermally degradable component of natural fibers [10].

Nanoparticles are gaining more importance in recent years to render novel properties to wood plastic composites [11,12]. Nanosilica is one of the most promising nanoparticles due to numerous positive effects it provides for composites, e.g., cost effectiveness, nontoxicity, environmental-friendliness, and improved thermal and mechanical performance [13, 14]. Low amounts (1-2 wt.%) of nano silica were reported by [15] to increase some of the mechanical properties of rice husk flour/polypropylene composites, whereas the higher amounts of the mentioned nanomaterial (3-4 wt.%) improved the composites water absorption. The incorporation of nano-montmorilonite and nanosilica in to rice straw/ polypropylene composites could enhance tensile and flexural moduli; however, the impact strength was considerably reduced [16].

To the best of the authors' knowledge, this is the first study reporting the synergistic effects of alkali and nanosilica treatments on the overall properties of bagasse/recycled polypropylene nanocomposites. A wide range of analyses including physical and mechanical tests as well as SEM, FTIR, TGA, and DSC were conducted to fully understand and analyze the mentioned structure-property relationships.

EXPERIMENTAL

Material

The bagasse fiber (sugarcane residue) was provided from Khuzestan Dash Laleh Nasr Co., Iran. Polypropylene (PP) grade V30G was purchased from Maroon Petrochemical Co., Iran, and Maleic anhydride grafted ploypropylene (MAPP), as the compatibiliser, was purchased from Aria Polymer Pishgam, Iran. The technical specifications of the mentioned polymers are given in Table 1.

Nanosilica was provided from Degussa Co., Germany, and sodium hydroxide (99%) was purchased from Merck Co., Germany.

Table 1. Polymer specifications.

Material	Melt flow index (g/10min)	Density (g/cm^3)
Polypropylene-V30G	16	0.9
Maleic anhydride grafted Polypropylene	10	0.95

Preparation of bagasse fibers

The fibers first underwent a one-hour soak in hot water. They were then left to air-dry for a period of 72 hours. After this, the fibers were placed in an oven and dried at a temperature of 103°C for 24 hours. Following this drying process, the fibers were fed into a rotary chipper for further processing. From the resulting material, the 30-100 mesh size fraction was selected to be used in subsequent experiments.

For mercerization treatment, the fibers were immersed in a 5% sodium hydroxide solution at room temperature. After 2 hours, the fibers were washed and rinsed with distilled water. The washed fibers were then air-dried for a period of three days. After the fibers underwent the final oven-drying at 103°C for 24 hours, the treated bagasse fibers were packed and sealed in plastic bags for any further processing steps.

Production of recycled polypropylene

The polypropylene extrusion process was conducted at a temperature of 190°C with a single screw extruder having 5 thermal zones manufactured by Pouya Polymer Amirkabir Iran Co., Iran. The resulting material was cut in to recycled PP granules. These granules were then pulverized and sealed in plastic bags for further steps.

Composite fabrication

The composite materials were first placed in an oven and dried at a temperature of 103°C for 12 hours. After the drying process, the materials were sealed in plastic bags. This was done to prevent any potential changes in the moisture content of the materials.

The dried materials were then weighed precisely to the nearest 0.001 gram and mixed based on the weight percentages specified in Table 2. This mixing process was carried out in a rotary mixer, manufactured by Santam Co. in Iran, for a duration of 5 minutes.

The resulting mixed material was then placed into a mold with dimensions of 28×28×1.3 cm. This mold-filled mixture was then pressed using a hydraulic hot press, also provided by Santam Co. in Iran. The pressing was done at a temperature of 185°C, under a pressure of 35 bar, for a duration of 18 minutes.

Characterization of composite materials

Physical properties

Water absorption (WA) and thickness swelling (TS)

Table 2. Composite formulations.

Samples code	Fiber content (wt.%)	PP content (wt.%)	Coupling agent content (wt.%)	Treatment	Nano (wt.%)
PMB	50	48	2	Untreated	0
PMBA	50	48	2	treated	0
PMBNs	50	44	2	Untreated	4
PMBANs	50	44	2	treated	4

characterizations were performed on the samples in accordance with ASTM D7031-11 standard specifications. These tests were conducted with 5 replicate samples and calculated based on Equations 2 and 3.

$$\%WA = \left(\frac{m_w - m_d}{m_d}\right) \times 100 \quad (2)$$

Where: m_w and m_d represent composites wet and oven-dried weights

$$\%TS = \left(\frac{t_w - t_d}{t_d}\right) \times 100 \quad (3)$$

Where: t_w and t_d represent composites wet and oven-dried thicknesses

Mechanical properties
The unnotched impact and bending strengths of the samples were evaluated following the ASTM D256 and ASTM D790 standard test methods, respectively. These tests were carried out, using an Instron testing machine model 4489 with five replicate samples for each measurement.

Fourier transform infrared spectroscopy (FTIR)
The untreated and alkali treated fibers were analyzed by a Fourier transform infrared spectroscopy system. Specifically, a Tensor 27 IR spectrophotometer manufactured by Bruker Co. in Germany was used for this analysis. The FTIR scans were performed over a transmittance range of 4000 to 370 cm^{-1}.

Scanning electron microscopy (SEM)
The fractured surfaces of the composites were scanned using scanning electron microscopy (SEM). This test was carried out to study the fiber-polymer interfaces and also morphology of the treated and untreated composites. The SEM instrument used was a MIRA III model, manufactured by Tescan Co and the fractured surfaces were coated with a thin layer of gold before scanning.

Thermogravimetric properties (TGA)
Thermogravimetric analysis was carried out on the samples using a thermal gravimetric analyzer Model STA 504, manufactured by Bahr, Germany. During the TGA analysis, the composite samples were heated from 25°C to 600°C at a rate of 10°C per minute.

Differential scanning calorimetry (DSC)
The composite samples were analyzed using a Q600 differential scanning calorimeter (DSC) from TA Instruments, USA. Each sample, weighing 15 ± 0.2 mg, underwent the DSC characterization. The DSC analysis was conducted under a nitrogen atmosphere with heating rate of 10°C/min. As the endothermic polymer melting peak covers the exothermic peak of the initial stage of wood degradation, all the measurements were conducted twice. Thus, the measurements are for the second runs, i.e., second heating run after cooling step, where the exothermic effect does not repeat.

Statistical analysis
The statistical analysis was done using a completely randomized factorial design, which was implemented using SPSS software. One-way analysis of variance (ANOVA) was employed to analyze the data. The means were then grouped via Duncan's Multiple Range Test (DMRT) at 95% confidence level.

RESULTS AND DISCUSSION

Physico-mechanical Properties

Water absorption and thickness swelling
There is similar WA and TS trends in the studied composite formulations (Figure 1). The untreated bagasse fiber composites (PMB) presented the highest WA rates (8%) as a result of the hydrophilic nature of cellulosic bagasse fibers[17]. The incorporation of 4 wt.% nanosilica in to the composites (PMBNs) resulted in a slight reduction of WA and TS rates. Nanosilica prevents from water ingress in to composites due to its barrier properties[18]; it also fills the micro and nano

voids existing in the composite matrix, leading to reduced physical properties[11]. Mercerization could slightly reduce WA and TS rates in PMBA composites vs. the untreated PMB ones. The reason behind this is the reduction of polar hydroxyl moieties brought about by alkali treatment which entails stronger chemical affinity between the now less polar bagasse fibers and the apolar polypropylene matrix[19]. PMBANs composite exhibited the lowest WA (7%) and TS rates (<4%). Except for WA and TS rates of PMBA composites, there were significant differences between the WA and TS rates of PMBANs and those of all the other composite formulations.

Flexural strength

Flexural strength presented a statistically significant improvement in PMBA composites vs. the reference ones (Figure 2). Gwon reported that mercerization improvements the mechanical performance of natural fiber composites by both enhanced mechanical interlocking and chemical bonding[20]. Nanosilica had almost no statistically significant effect on the composites; the weak chemical affinity of nanosilica and polyproplene and also the agglomeration of the given nanoparticles brought about by Van der Waals and electrostatic forces can play a role in this phenomenon[21]. PMBANS composites (vs. PMBA ones) showed a very slight increase in flexural strength. This can be due to the formation of a more homogeneous fiber-polymer interaction[22-24].

Modulus of elasticity

The MOE of PMBNs composites is almost identical to that of the reference ones showing no significant improvements (Figure 3). Figure 3 also displays

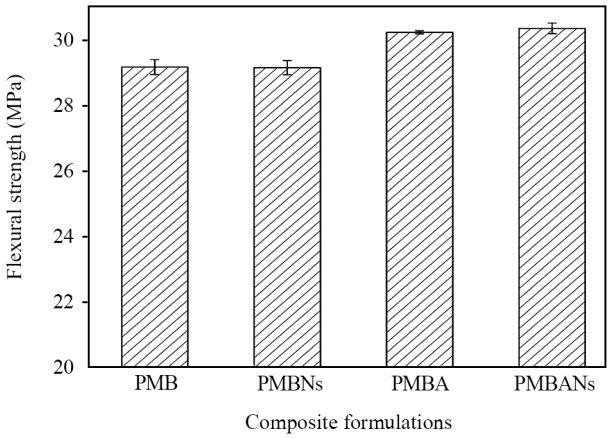


Figure 2. Flexural strength of composite formulations.

enhanced MOE values for the mercerized PMBA samples (vs. the reference); however, the long error bar in PMBA may indicate that the values are more spread out and less reliable. The MOE of PMBANs composites is slightly higher than PMBA ones; this can be relative to the improved interfacial adhesion due to the addition of nanosilica and the entailing better stress transfer in the polymer matrix [25].

Impact strength

The impact strength values of PMBNs and PMBANs composites did not show any significant difference with that of the reference formulation (Figure 4). The restriction of polymer chain movements due to the effect of nanoparticles may undermine the ability of composites to absorb the applied impact energy. Moreover, the presence of nondispersed fiber bundles and voids would adversely affect impact strength [26-28]. Archival publications present contradictory findings regarding the impact strength of wood-plastic composites, indicating a need for further

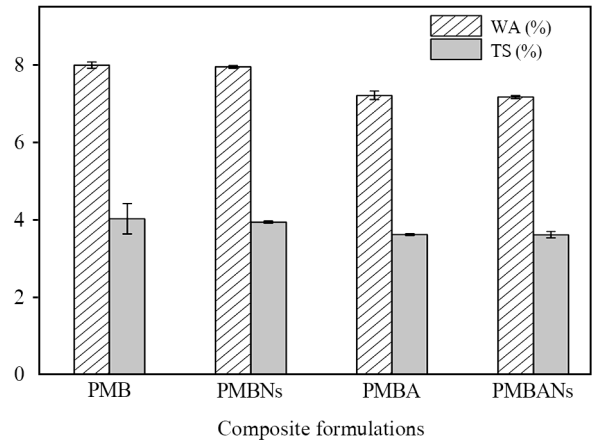


Figure 1. Water absorption and thickness swelling of the studied composites.

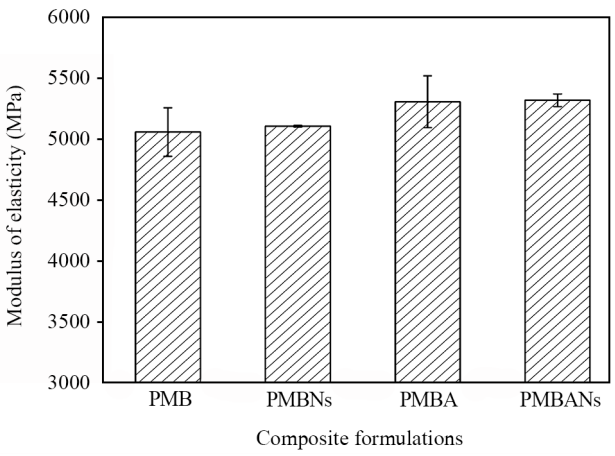


Figure 3. Modulus of elasticity of various samples.

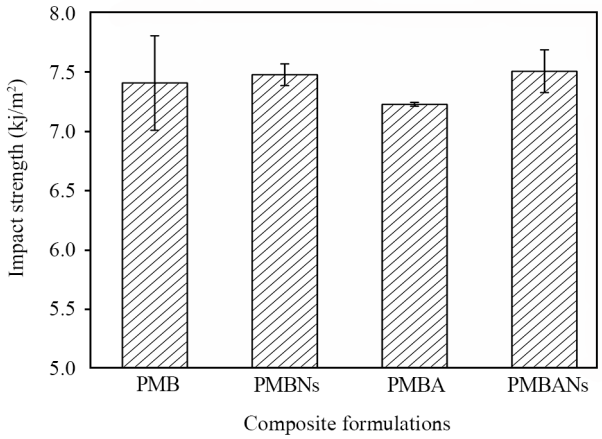


Figure 4. Impact strength of composite formulations.

investigation. Additionally, the unnotched impact strength test is significantly influenced by the surface properties of composite samples; in cases where a hard and rigid substance is present on the sample surface, an increase in impact strength is anticipated [29,30]. Mercerization leads to strong but rigid fiber-polymer phases, and therefore the composites would be fractured at relatively lower impact energy rates [29]. Consequently, the PMBA composites exhibited the lowest impact strength (7.23 kJ/m).

FTIR results

The infrared spectrum (Figure 5 and Table. 3) indicates that the band at 3440 cm^{-1}, which corresponds to the stretching of hydroxyl (-OH) groups in the bagasse fibers, has a lower intensity of absorbance in the treated fibers vs. the untreated ones. This is due to a reduction in the number of bagasse hydroxyl groups after NaOH treatment [31,32]. The C-H stretching of aromatic methyl and methylene moieties present in lignin appeared as the strong peaks at 2921 cm^{-1} [33]. Mercerization had trace effects on the removal of lignin components in the fibers, as the peaks did not show significant differences between the treated and untreated bagasse fibers. The vibrational stretching of unconjugated carbonyl functional moieties (C=O) existing in hemicelluloses is detected with the absorption band observed at 1736 cm^{-1} [34]. Based on Figure 5, this band has disappeared in the alkali-treated fibers, demonstrating the removal of hemicellulose components by this treatment [35,36]. The peak at 1432 cm^{-1} is the stretching of C-H bonds in the amorphous and crystalline regions of the cellulose chains. After mercerization, this peak has shifted to 1429 cm^{-1} and also increased in intensity. This can be ascribed to the release of C-H groups from the fiber surfaces due to the alkali impact [37]. The absorption peak observed at 1047 cm^{-1} is attributed to the stretching vibrations of the C-C and C-O bonds present in hemicellulose xylan, as well as the C-O-C bonds in the glycosidic linkages of hemicellulose components [38]. This peak has exhibited a remarkable increase in intensity following the alkali treatment indicating a marked increase in intensity following the alkali treatment. The observed increase in the intensity of the 1047 cm^{-1} peak can be attributed to the fibrillation phenomenon induced by the NaOH treatment. This chemical treatment has the effect of opening up the interwoven cellulose and hemicellulose chains, thus creating the aforementioned stretching bonds (i.e., C-C, C-O, and C-O-C) more accessible and prone to absorb the infrared light during the FTIR analysis [39].

Scanning electron microscopy

The fracture surface of the PMB sample (Figure 6a) exhibits some gaps and cavities, indicating fiber pull-outs. This suggests a weak interfacial adhesion between the fibers and the matrix leading to impaired mechanical properties of the PMB composites.

While Figure 6b shows that nanosilica has agglomerated in some areas holding the potential to adversely affect the properties of the PMBNS composites, the fracture surfaces also reveal some positive attributes. Although a few cavities are

Table 3. FTIR analysis of fibres.

Frequency Number (cm^{-1})	Functional group	Reference
3440	Vibrations of the hydrogen-bonded hydroxyl group	[35]
2921	C-H stretching in aromatic methoxyl group and methylene group	[55]
1736	Acetyl and uronic ester groups attached to hemicellulose	[56]
1605	OH bending of water in hemicellulose	[35]
1462	The C-H bending and C-O stretching frequencies of hemicellulose	[37]
1248	The acetyl groups of the hemicelluloses	[35]
1047	C-O and C-C stretching band of xylanes C-O-C stretching of the glycosidic linkage in hemicellulose	[57]
893	The C-H bending of amorphous and crystalline cellulose	[39]
829	CH-bending vibration	[58]

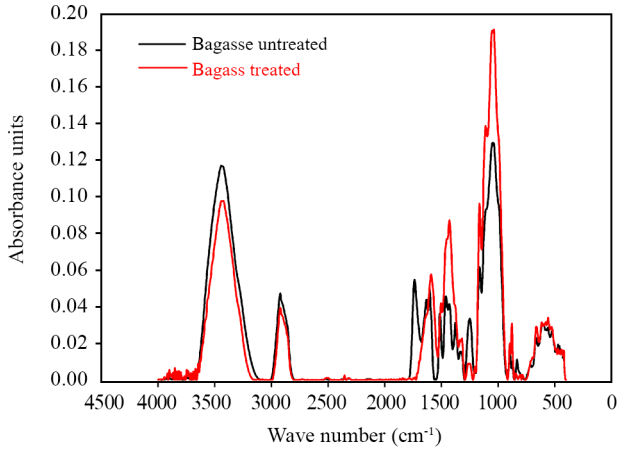


Figure 5. FTIR spectra of mercerized and untreated bagasse fibers.

present due to fiber pull-outs, there are also instances of fiber fractures, which indicate better fiber-polymer entanglement in the PMBNS samples; this corroborates the enhanced physical and mechanical properties of the mentioned composites.

As observed in Figure 6c, the PMBA composites display a reduced number and size of cavities caused by fiber pull-outs, compared to the PMB formulation. This indicates better bonding between the fibers and the polymer in the PMBA composites than in the PMB ones. Additionally, Alkali fibrillation of the fibers in the PMBA composites could increase the accessible hydroxyl groups on fiber surfaces, leading to improved bonding of fibers and the incorporated coupling agent present in the given composites [40].

Figure 6d illustrates a fairly uniform and smooth surface, indicating good fiber encapsulation by the polymer and adhesion between the fiber and polymer phases. There are almost no visible gaps or cavities between the two components, suggesting a well-integrated composite structure. As also seen in Figure 6d, the presence of fiber fracture areas suggests that the incorporation of nanosilica particles has enhanced the mechanical and interfacial characteristics of the material.

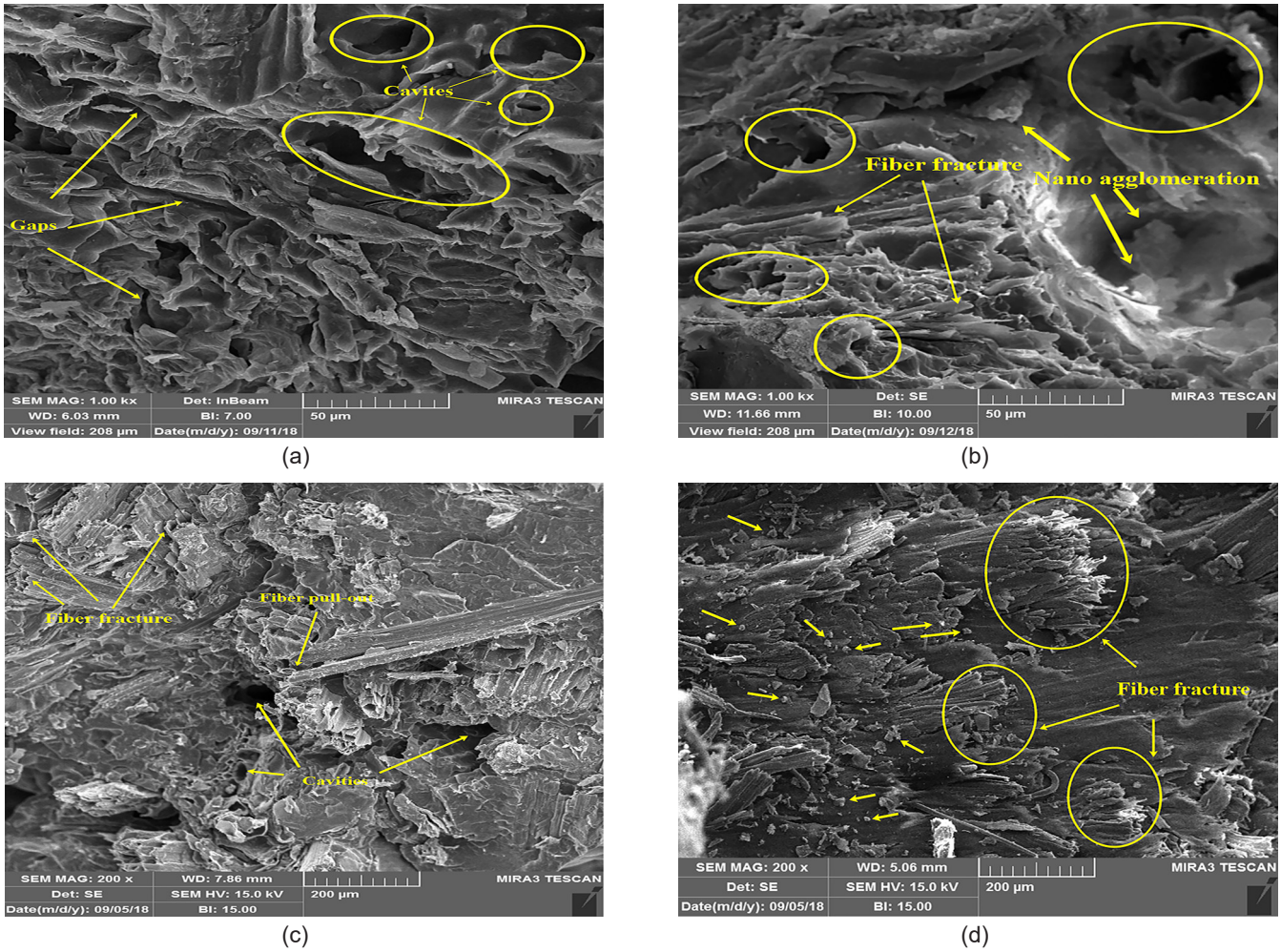


Figure 6. SEM micrograph of (a) PMB, (b) PMBNs, (c) PMBA, (d) PMBANs composites.

Table 4. TGA analysis of bagasse fiber/polypropylene composites.

Sample code	T_i	T_{d1}	T_{d2}	T_{10} (°C)	T_{max} (°C)	(°C) T_{50}	Char (%)
PMB	242.1	321	421.5	320.1	448.3	450.1	12.5
PMBA	242	321	421.4	319.7	448.3	450	11.8
PMBNs	242.1	320.5	433.7	321.6	448.5	449.5	14.6
PMBANs	242.3	322.1	447.2	323.2	449	449.1	14.7

T_i=initial decomposition temperature, T_{d1}=first decomposition temperature, T_{d2}=second decomposition temperature, T_{10}=temperature at 10% weight loss, T_{max}=temperature at maximum degradation, T_{50} = temperature at 50% weight loss.

Thermal results

TGA

As indicated in Table 4, the thermal degradation of bagasse fibers (T_i) initiated at about 240ºC [41], which is due to the low thermal degradation threshold of holocellulose polymers and lignin. The degradation temperature of hemicellulose is between 150-350ºC, cellulose is around 275-350ºC, and lignin starts to thermally degrade at 250-500ºC [42]. Therefore, the primary contributors to the initial stage of thermal degradation in the given composites are cellulose, hemicellulose, and lignin polymers [43]. Mercerization partly reduced the thermal properties of PMBA formulation, as a result of the decreased lignin content. TGA analysis also infers that the addition of nanosilica by itself can somewhat increase the T_{d2}, T_{10}, and T_{max} of PMBNs composites versus those of the PMB and PMBA formulations, whereas T_i and T_{50} were negatively affected, which needs to be further studied.

Several mechanisms have been proposed to explain the enhanced thermal stability observed in the studied nanocomposites. First the silicate layers of the nanoparticles elongate the twisted pathways, hindering the diffusion of heat and combustible volatiles [44, 45], and also the addition of nanosilica results in the formation of a protective char layer over the composite materials. This delays the burning process of the underlying layers, bringing about enhanced thermal properties for the studied composite formulation [46]. Last but not least, the nanosilica particles limit the chain mobility of the matrix polypropylene; this interaction-induced restriction of chain mobility improves the overall thermal properties of the given formulation [47].

Except for T_{50}, the combined treatment of mercerization and nanosilica exhibited a synergistic effect, leading to an increase in the T_i, T_{d1}, T_{d2}, T_{10}, T_{max}, and char yield rates of PMBANs formulation.

DSC

The findings (Table 5) suggest that the process of mercerization may have a minor negative impact on the thermal properties of PMBA composites. This is likely due to the presence of lignin, which functions as a binding agent between the fibers. The lignin acts as a barrier, preventing the sodium hydroxide used in the mercerization process from fully ingressing these areas of the composite material[48,49]. Higher amounts of alkali were found to remarkably impair the thermal properties. This is due to the combined effects of the transformation of cellulose and changes in crystallinity [50,51]. Additionally, the blocking effect of the wood fibers on the polymer crystallization could lead to the lower crystallinity rates observed in WPCs [50]. The DSC results showed that nanosilica particles act as nucleating agents, promoting crystal growth and likewise, increasing the crystallization and strength of the composites. The addition of nanosilica strengthened the bond between the polyethylene matrix and bagasse fibers, and also incrementally improved the crystallinity and thermal properties of the given nanocomposite [52]. The DSC analysis also indicated that the combined nanosilica and alkali treatments could noticeably improve the overall thermal indices mentioned in Table 4. Othman postulated that the partial dissolution of wax, oil, lignin, and hemicellulose is responsible for such changes [53]. Vidyashri et al. (2019) reported that the accessibility of nanosilica to the alkali-exposed cellulose hydroxyl

Table 5. DSC analysis of bagasse fiber/polypropylene composites.

Sample code	T_m(°C)	T_c(°C)	X_c (%)	ΔH_c (j/g)	ΔH_m (j/g)
PMB	171.2	121.5	30.1	65.1	60.1
PMBA	170.0	121.2	30.1	64.9	59.5
PMBNs	171.2	121.3	29.5	64.6	59.8
PMBANs	171.5	124.9	31.4	66.1	60.4

groups could lead to enhanced thermal performance of the studied nanocomposites [54].

CONCLUSION

This study reports the effects of nanosilica and alkali treatment on the overall properties of recycled polypropylene/bagasse composites. WA and TS of the nanocomposites improved due to the blocking properties of nanosilica platelets. Furthermore, alkaline treatment reduced the hydroxyl groups present in bagasse fibers, as confirmed by FTIR analysis, and further improved the water resistance. Unlike PMBNs composites, flexural strength and modulus of elasticity of PMBANs enhanced due to the modification of the bagasse fiber surfaces by alkali. The impact strengths of PMBA composites were lower than those of reference ones due to the impaired impact energy absorption of the strong fiber-polymer interfaces in the former composites. The impact strength values of PMBNs and PMBANs composites did not show significant differences with that of the reference formulation. The thermal properties of PMBA and PMBNs had no significant improvements whereas PMBANs composites showed significantly better overall thermal properties. The results of this study indicate that combined nanosilica-alkali treatment of natural fiber polymer composites holds a promising potential to synergistically valorize the structural properties of the given bio-nanomaterials, transforming them into high-performance, and likewise eco-friendly materials for various industrial purposes.

FUNDING DECLARATION

This research was funded by the authors, and no other organization was involved in this respect.

CONFLICTS OF INTEREST

There is no known conflict of interest.

REFERENCES

1. Nadali E, Karimi A, Tajvidi M, Naghdi R (2010) Natural durability of a bagasse fiber/ polypropylene composite exposed to rainbow fungus (coriolus versicolor). J Reinf Plast Compos 29: 1028-1037
2. Naghdi R, Karimi AN, Jahan Latibari A, Hamzeh Y, Mirshokraie SA, Nadali E (2013) Biological removal of chloro-organic compounds from bagasse soda pulp bleaching effluent by Coriolus versicolor. Global NEST J 15: 29-36
3. Naghdi R, Nadali E, Younesi Kordkheili H (2015) Evaluation of pulp and paper properties obtained from maple juvenile wood through organosolv alcohol method catalyzed by calcium and magnesium salts. Iran J Wood Paper Ind 6: 31-40
4. Nadali E, Layeghi M, Ebrahimi G, Naghdi R, Jonoobi M, Khorasani MM, Mirbagheri Y (2018) Effects of multiple extrusions on structure-property performance of natural fiber high-density polyethylene biocomposites. Mat Res 21
5. Nadali E, Tajvidi M, Naghdi R (2021) Effects of fungal biodegradation on structure–property relationships of medium density fibre board and hybrid polypropylene composite made from sugar-cane residue. Int Wood Prod J 12: 152-163
6. Naghdi R, Karimi A, Latibari A, Mirshokrayi S (2009) Evaluation of the effect of rainbow fungus (coriolus versicolor) bleach plant effluent color reduction. Iran J Natural Resources 61: 989-995
7. Dittenber DB, GangaRao HVS (2012) Critical review of recent publications on use of natural composites in infrastructure. Compos Part A Appl Sci Manuf 43: 1419-1429
8. Mohanty AK, Misra M, Drzal LT (2001) Surface modifications of natural fibers and performance of the resulting biocomposites: An overview. Composite Interfaces 8: 313-343
9. Saxena M, Pappu A, Haque R, Sharma A (2011). Sisal fiber based polymer composites and their applications. In: Cellulose Fibers: Bio- and Nano-Polymer Composites. Ed(s): S. Kalia, B.S. Kaith, I. Kaur, Springer, pp: 589-659
10. Naghdi R (2021) Advanced natural fibre-based fully biodegradable and renewable composites and nanocomposites: A comprehensive review. Int Wood Prod J 12: 178-193
11. Yonesi Korekhili H, Naghdi R, Amiri M (2015) The effect of nanoclay on physicochemical, mechanical and thermal properties of new urea-glyoxal resin. Iran J Wood Paper Ind 6: 133-143
12. Yousefi S, Kartoolinejad D, Naghdi R (2017) Effects of priming with multi-walled carbon

nanotubes on seed physiological characteristics of Hopbush (DodonaeaviscosaL.) under drought stress. Int J Environ Stud 74: 528-539
13. Nejat T, Jalalinezhad P, Hormozi F, Bahrami Z (2019) Hydrogen production from steam reforming of ethanol over Ni-Co bimetallic catalysts and MCM-41 as support. J Taiwan Ins Chem Eng 97: 216-226
14. Shariati M, Farzi G, Dadrasi A (2015) Mechanical properties and energy absorption capability of thin-walled square columns of silica/epoxy nanocomposite. Constr Build Mater 78: 362-368
15. Nourbakhsh A, Farhani Baghlani F, Ashori A (2011) Nano-SiO_2 filled rice husk/polypropylene composites: Physico-mechanical properties. Ind Crops Prod 33: 183-187
16. Ashori A (2013) Effects of nanoparticles on the mechanical properties of rice straw/ polypropylene composites. J Compos Mater 47: 149-154
17. Nadali E, Naghdi R (2022) Effects of multiple extrusions on structure–property relationships of hybrid wood flour/poly (vinyl chloride) composites. J Thermoplast Compos Mater 35: 1076-1093
18. Jiang J, Mei C, Pan M, Cao J (2020) Improved mechanical properties and hydrophobicity on wood flour reinforced composites: Incorporation of silica/montmorillonite nanoparticles in polymers. Polymer Composites 41: 1090-1099
19. Gunwant D (2024) Moisture resistance treatments of natural fiber-reinforced composites: a review. Compos Interfaces 31: 979-1047
20. Gwon JG, Lee SY, Chun SJ, Doh GH, Kim JH (2010) Effect of chemical treatments of wood fibers on the physical strength of polypropylene based composites. Korean J Chem Eng 27: 651-657
21. Ke YC, Stroeve P (2005) Polymer-layered silicate and silica nanocomposites. In: Polymer-layered silicate and silica nanocomposites, Elsevier, pp: 119-209
22. Amjad A, Abidin MSZ, Alshahrani H, Rahman AAA(2021) Effect of fibre surface treatment and nanofiller addition on the mechanical properties of flax/PLA fibre reinforced epoxy hybrid nanocomposite. Polymers 13: 3842
23. Ramos VD, da Costa HM, Soares VLP, Nascimento RSV (2005) Modification of epoxy resin: a comparison of different types of elastomer. Polym Test 24: 387-394
24. Okolie J, Nanda S, Dalai AK, Kozinski JA (2021) Chemistry and specialty industrial applications of lignocellulosic biomass. Waste Biomass Valoriz 12: 2145-2169
25. Naghdi R, Nejat T (2023) Effects of organically-modified montmorillonite and alkalinization on physical, mechanical, chemical, morphological, and thermal properties of wheat straw/recycled polypropylene nanocomposites. J Compos Mater 57: 2127-2144
26. Landel RF, Nielsen LE (1993) Mechanical properties of polymers and composites, CRC Press
27. Yadav SM, Yusoh KB (2019) Subsurface mechanical properties and subsurface creep behaviour of modified nanoclay-based wood–plastic composites studied by nanoindentation. Polym Bull 76: 2179-2196
28. Khanjanzadeh H, Tabarsa T, Shakeri A, Omidvar A (2011) Effect of organoclay platelets on the mechanical properties of wood–plastic composites formulated with virgin and recycled polypropylene. Wood Mater Sci Eng 6: 207-212
29. Bartos A, Utomo BP, Kanyar B, Anggono J, Soetaredjo FE, Móczó J, Pukánszky B (2020) Reinforcement of polypropylene with alkali-treated sugarcane bagasse fibers: Mechanism and consequences. Compos Sci Technol 200: 108428
30. Bledzki AK, Mamun AA, Volk J (2010) Physical, chemical and surface properties of wheat husk, rye husk and soft wood and their polypropylene composites. Compos Part A Appl Sci Manuf 41: 480-488
31. Jonoobi M, Harun J, Shakeri A, Misra M, Oksman K (2023) Chemical composition, crystallinity, and thermal degradation of bleached and unbleached kenaf bast (Hibiscus cannabinus) pulp and nanofibers. BioResources 4: 626-639
32. Perrone OM, Colombari FM, Rossi JS, Moretti MMS, Bordignon SE, Nunes CCC, Gomes E, Boscolo M, Da-Silva R (2016) Ozonolysis combined with ultrasound as a pretreatment of sugarcane bagasse: Effect on the enzymatic saccharification and the physical and chemical characteristics of the substrate. Bioresour Technol 218: 69-76
33. Ma Z, Wang J, Zhou H, Zhang Y, Yang Y, Liu X, Ye J, Chen D, Wang S (2018) Relationship of thermal degradation behavior and chemical

structure of lignin isolated from palm kernel shell under different process severities. Fuel Process Technol 181: 142-156
34. Chen C, Luo J, Qin W, Tong Z (2014) Elemental analysis, chemical composition, cellulose crystallinity, and FT-IR spectra of Toona sinensis wood. Monatsh Chemie 145: 175-185
35. Kabir MM (2012) Effects of chemical treatments on hemp fibre reinforced polyester composites, PhD Thesis, University of Southern Queensland
36. Raju JSN, Depoures MV, Kumaran P (2021) Comprehensive characterization of raw and alkali (NaOH) treated natural fibers from Symphirema involucratum stem. International Journal of Biological Macromolecules 186: 886-896
37. Peng F, Ren J-L, Xu F, Bian J, Peng P, Sun R-C (2010) Fractional study of alkali-soluble hemicelluloses obtained by graded ethanol precipitation from sugar cane bagasse. J Agric Food Chem 58: 1768-1776
38. Sun S-F, Yang H-Y, Yang J, Shi Z-J (2022) The effect of alkaline extraction of hemicellulose on cocksfoot grass enzymatic hydrolysis recalcitrance. Ind Crops Prod 178: 114654
39. Łojewska J, Miśkowiec P, Łojewski T, Proniewicz LM (2005) Cellulose oxidative and hydrolytic degradation: In situ FTIR approach. Polym Degrad Stabil 88: 512-520
40. Wang F, Zhou S, Yang M, Chen Z, Ran S (2018) Thermo-mechanical performance of polylactide composites reinforced with alkali-treated bamboo fibers. Polymers 10: 401
41. El-Shekeil YA, Sapuan SM, Khalina A, Zainudin ES, Al-Shuja'a OM (2012) Effect of alkali treatment on mechanical and thermal properties of Kenaf fiber-reinforced thermoplastic polyurethane composite. J Therm Anal Calorim 109: 1435-1443
42. Hidalgo D, Castro J, Díez D, Martín-Marroquín J, Gómez M, Pérez E (2023) Torrefaction at low temperature as a promising pretreatment of lignocellulosic biomass in anaerobic digestion. Energy 263: 125822
43. Budiyantoro C, Yudhanto F (2024) Comparative analysis of cellulose, hemicellulose and lignin on the physical and thermal properties of wood sawdust for bio-composite material fillers. Revue des composites et des matériaux avancés 34: 109-116
44. Nabipour H, Rohani S (2024) Flame retardant properties of polymer nanocomposites based on new layered structure nanoparticles. In: Flame retardant nanocomposites, Woodhead Publishing, pp 117-158
45. Rosa MF, Chiou B, Medeiros ES, Wood DF, Williams TG, Mattoso LHC, Orts WJ, Imam SH (2009) Effect of fiber treatments on tensile and thermal properties of starch/ethylene vinyl alcohol copolymers/coir biocomposites. Bioresour Technol 100: 5196-5202
46. Khosravian B (2010) Studying mechanical, physical, thermal and morphological characteristics of hybrid composites of polypropylene/wood flour/wollastonite. Master's Thesis, University of Tehran, Tehran, Iran
47. Luyt A, Dramićanin MD, Antić Ž, Djoković V (2009) Morphology, mechanical and thermal properties of composites of polypropylene and nanostructured wollastonite filler. Polym Test 28: 348-356
48. Nurazzi NM, Asyraf MRM, Rayung M, Norrrahim MNF, Shazleen SS, Rani MSA, Shafi AR, Aisyah HA, Radzi MHM, Sabaruddin FA, Ilyas RA, Zainudin ES, Abdan K (2021) Thermogravimetric analysis properties of cellulosic natural fiber polymer composites: A review on influence of chemical treatments. Polymers 13: 2710
49. Zhang J, Jiang DD, Wilkie CA (2006) Thermal and flame properties of polyethylene and polypropylene nanocomposites based on an oligomerically-modified clay. Polym Degrad Stabil 91: 298-304
50. Chen H, Zhang W, Wang X, Wang H, Wu Y, Zhong T, Fei B (2018) Effect of alkali treatment on wettability and thermal stability of individual bamboo fibers. J Wood Sci 64: 398-405
51. Šoštarić T, Petrović M, Stojanović J, Marković M, Avdalović J, Hosseini-Bandegharaei A, Lopičić Z (2022) Structural changes of waste biomass induced by alkaline treatment: the effect on crystallinity and thermal properties. Biomass Conv Bioref 12: 2377-2387
52. Parvinzadeh M, Moradian S, Rashidi A, Yazdanshenas M-E (2010) Surface characterization of polyethylene terephthalate/silica nanocomposites. Appl Surf Sci 256: 2792-2802
53. Othman N, Ismail H, Mariatti M (2006) Effect of compatibilisers on mechanical and thermal

properties of bentonite filled polypropylene composites. Polym Degrad Stabil 91: 1761-1774
54. Vidyashri V, Lewis H, Narayanasamy P, Mahesha GT, Bhat KS (2019) Preparation of chemically treated sugarcane bagasse fiber reinforced epoxy composites and their characterization. Cogent Eng 6: 1708644
55. Xiao B, Sun XF, Sun RC (2001) Chemical, structural, and thermal characterizations of alkali-soluble lignins and hemicelluloses, and cellulose from maize stems, rye straw, and rice straw. Polym Degrad Stabil 74: 307-319
56. Liu Q, Zhong Z, Wang S, Luo Z (2011) Interactions of biomass components during pyrolysis: A TG-FTIR study. J Anal Appl Pyrol 90: 213-218
57. Wang K, Jiang J-X, Xu F, Sun R-C, Baird M-S (2010) Influence of steam pressure on the physico-chemical properties of degraded hemicelluloses obtained from steam-exploded Lespedeza stalks. BioResources 5: 1717-1732
58. Tan SJ, Supri AG (2016) Properties of low-density polyethylene/natural rubber/water hyacinth fiber composites: the effect of alkaline treatment. Polym Bull 73: 539-557